LA-UR- 93-2140

Title: MEASUREMENTS OF SPATIAL AND FREQUENCY COHERENCE OF AN EQUATORIAL HF PATH DURING SPREAD-F

Author(s): T. Joseph Fitzgerald, SST-7
Paul E. Argo, SST-7
Robert C. Carlos, SST-7

Submitted to: TENERP Conference
Monterey, CA
June 21-24

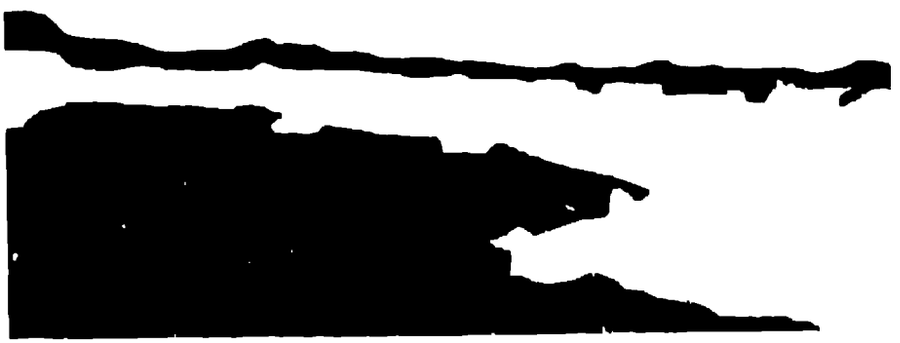

Los Alamos
NATIONAL LABORATORY

Measurements of Spatial and Frequency Coherence of an Equatorial HF Path during Spread-F

T. J. Fitzgerald, P. E. Argo, and R. C. Carlos

Atmospheric Sciences Group
Mail Stop D466
Los Alamos National Laboratory
Los Alamos, New Mexico 87545

Abstract

In August 1990, we set up an hf path on the equatorial path between Maloelap Atoll and Bikini Atoll. This path, which had a range of 702 km, reflected in the ionosphere approximately 100 km north of the Altair radar location on Kwajalein. Transmitters at Maloelap broadcasted four cw tones within bandwidth of either 4 kHz, 9 kHz, or 70 kHz to be used to determine frequency coherence and also a phase-coded pseudo random sequence with a bandwidth of 60 kHz (channel probe) to be used to determine time delay spread. A spatial array of antennas was deployed at Bikini to measure spatial and frequency coherence using the cw broadcasts. The system was run in the post-sunset time period over two weeks during which almost every night showed significant degradation due to spread F resulting in rapid fading, decreased spatial and frequency coherence, and increased time delay spread. Doppler spreads of greater than 20 Hz were not uncommon, and the spatial correlation distances and frequency coherence bandwidths became so small (50 meters and 1 kHz respectively) that we had to readjust the experiment. Measurements taken by the Altair incoherent scatter radar and the CUPRI 50 MHz coherent scatter radar indicate that although the bistatic hf channel is affected by the large scale plume structures, most of the "damage" is done by the bottomside spread F.

Introduction

In conjunction with the NASA sponsored equatorial rocket campaign conducted in August, 1990, at the Kwajalein Missile Range, we set up an hf (10.2 MHz) radio path between Maloelap Atoll (8.700 N, 171.230 E) and Bikini Atoll (11.630 N, 165.540 E). The local time at all stations is eleven hours offset from UT. The path, which had a range of 702 km, reflected in the ionosphere approximately 100 km north of the Altair (155 MHz) radar and the Cupri (50 MHz) radar location. Figure 1 shows the experimental geometry. Transmitters at Maloelap broadcasted four cw tones within bandwidths of 4/9/70 kHz to be used to determine frequency coherence and also a phase coded pseudorandom sequence with a bandwidth of 60 kHz (channel probe) to be used to determine time delay spread. A spatial array of eight antennas (figure 2) was deployed at Bikini to measure spatial coherence and angle of arrival using the cw transmissions. Receivers also monitored the multiple frequency cw broadcasts and the channel probe transmission. The system was run in the post sunset time period over two weeks during which almost every night showed significant degradation of the received signals associated with spread F resulting in rapid fading, decreased spatial and frequency coherence, and increased time delay spread. In this presentation, we concentrate on the cw results for the evening of Aug 10, 1990 (UT) for which data from the Altair radar (operated by SRI International) and the Cupri radar (operated by Cornell University) are available. Channel probe data were not available for this particular day.

Experiment

We employed two types of oblique hf sounders: cw- Doppler and a channel probe. The former consisted of four cw transmissions with the lowest frequency at 10.224 MHz and the other frequencies were initially offset by 10, 30, and 70 kHz higher. In the middle of the evening discussed in this paper we changes the frequency offsets to 1, 3, and 9 kHz. On following days we reduced the spacing further, to .5, 1.5, and 4 kHz. The cw tones were generated by four frequency synthesizers which were locked to the 10 MHz output of a Global Positioning Satellite (GPS) receiver. The outputs of the synthesizers were fed into four linear amplifiers. The amplified cw was combined in two pairs in order to feed two antennas.

Magnetic loops of 1 m diameter were used as the receive antennas for the cw transmissions; the planes of the loops were vertical and aligned in the direction of the transmitter. The cw transmissions were detected using either Collins S1 or Racal 6790 receivers operated in cw mode at a beat frequency of 200 Hz with a bandwidth of 200 Hz. The frequency of the receivers were locked to a rubidium clock. An array of eight such systems were deployed in a 'T' pattern with six elements normal to the ray path and three elements parallel to the ray path. The audio output of each receiver, which was operated without automatic gain control, was digitized at a rate of 600 Hz and stored. A receiver connected to each of the eight antennas monitored the transmission at the base frequency; an additional three receivers connected to one antenna monitored the transmissions at the upper three frequencies.

Power Spectra versus Time

Because of time variations in the index of refraction of the ionosphere and the altitude of the hf reflection point the phase of the received cw signal will change resulting in a small Doppler frequency shift of the transmission. Negative Doppler shifts correspond to increasing phase paths. The power spectra of the received signal will display peaks at the corresponding Doppler shift; multipath will appear as multiple peaks in the power spectra with different frequency shifts for each component. Our method of calculating the evolution of the Doppler power spectra is based on the short-term Fourier transform. One divides the total time series of data into smaller sub-intervals over which the spectra appear stable and calculates the spectrum during that sub-interval. The sub-window is then advanced some fraction of its length and a new power spectrum calculated. The results may be visualized in a three dimensional plot which shows power at a given frequency and time as a color

Figure 3 illustrates the evolution of the power spectra over a period of 7500 s beginning at 0741 (1840 LT) UT for channel 1. There are data gaps near 3000 s (~1931 LT), 4700 s (2000 LT)and 6750 s (2033 LT); there was a also manual gain change near 3000 s. The behavior of the power spectra was typical; initially there was a well defined peak (~2 Hz) corresponding to the nominal one hop reflection. The Doppler shift is caused by the post sunset rise of the F layer of the ionosphere which results from the electrodynamics of the equatorial regime. We also observe multihop as peaks with even greater negative Doppler shift. The Doppler shift decreased as the upward motion of the ionosphere slowed.

The quality of the power spectra changed radically after 3000 s; identifiable modes disappeared into a very broad spectrum indicating rapid fading. This change was associated with the onset of spread-F which is a complex phenomenon characterized by structuring of the ionosphere over scale sizes from 100 km to .1 m. Such structures at the hf reflection level will produce a strong scattering over a broad area rather than a specular reflection at a single point. Simultaneously, the ionospheric plasma, driven by neutral winds, drifts anti-sunward (eastward) at about 125 m/s. Scattering from structures in motion produces the Doppler spread. Figure 4 shows individual Doppler spectra, before the onset of spread F (750 s) and well into developed spread F (5750 s). Note the presence of the multiple hops with increasingly offset Doppler on the early spectra, and the broad smeared character (~20 Hz wide) of the later spectra.

Coherence versus Time

Figures 5 and 6 illustrate the evolution of the spatial and frequency coherence. We plot the magnitude of the mutual coherence between two selected channels versus Doppler frequency using a color scale. The coherence was calculated from the normalized magnitude of the cross spectrum averaged over frequency. In figure 5 we show the spatial coherence between channels 1 and 3 which were separated by 50 m along the ray path. Initially these channels were highly coherent; in fact, there was a high coherence across the whole array, approximately .5 km. After the onset of spread-F, there was a significant decrease in the mutual coherence even at 50 m separation. This was typical of the data that we obtained on other evenings; we later decreased the antenna separation to 25 m.
In figure 6 we show the effect on frequency coherence using data from channels 8 and 9 which were obtained from the same antenna but using transmissions frequencies separated by 10 kHz. The onset on spread-F is marked by a total loss of coherence between these channels. In fact, we changed the frequency separation to 1 kHz in the last segment of data (after 7000 s) and obtained some coherence between channels. Data obtained from the channel probe indicated time delay spreads of about 1 millisecond which is consistent with the cw measurements.

Comparison to Radar Results

The Altair radar was operated over the same time period as our cw experiment during which time it made a number of scans across and along the magnetic meridian. This data has been made available to us through the courtesy of Roland Tsunoda of SRI International and David Hysell of Cornell University. The radar measures electron density using incoherent scatter; if the beam is perpendicular to the magnetic field, it will be sensitive to coherent structures of 1 m wavelength. We note that the hf reflection point was approximately 100 km east of the magnetic meridian at the radar; the electron density at the hf reflection point corresponds to a value of 5.9 on the (log) ne scale.

An east-west scan beginning at 8:01:41 UT (1200 s on our time scale) showed a smooth ionosphere with no coherent structures, figure 7. This lack of structure is consistent with the highly coherent hf signals observed at early time. A similar scan, figure 8, beginning at 8:47:20 UT (4000 s) shows coherent returns from the bottomside ionosphere (below the hf reflection level) and from a plume reaching to high altitudes. The plume structure would have passed the hf reflection point approximately 1000 s earlier and is likely to have produced the complicated set of peaks in the

Doppler spectra observed between 2000 and 3000 s. An off- perpendicular scan beginning 9:15:07 (5600 s) (figure 9) shows a highly structured ionosphere at large scales; a later meridian scan showed coherent structure reaching to high altitudes We ascribe the broad Doppler at late time to these highly structured conditions.

Discussion

By using highly synchronized tranmitters and receivers we are able to measure not only the Doppler broadening created by equatorial irregularities, but also the spatial correlation distances and the frequency coherence bandwidth. The Doppler broadening changed from a few hundred millihertz to nearly 20 Hz, while the spatial correlation distance shrunk from greater than .5 kilometers to less than 50 meters. The frequency coherence bandwidth decreased from greater than 70 kHz to less than 1 kHz.

Our data shows that the presence of bottomside spread F is sufficient to significantly degrade the hf propagation channel. During the onset of spread F we can identify distinct propagation modes that we connect to discrete "plume" structures, but once the entire overhead ionosphere is filled with irregularities it is difficult to distinguish individual structures, even of such large structure.

Figure Captions

Figure 1) The experimental geometry for the NICARE II hf propagtion experiment. The hf transmitters were on Maloelap Atoll, the receivers were on Bikini Atoll. The Altair Radar and the CUPRI Radar were on Kwajalein.

Figure 2) The geometry of the receive antenna array on Bikini Atoll. The transverse spacings were from 25 meters to 450 meters. The longitudinal spacings were 50 to 150 meters. The magnetic loop antennas were all aligned in the plane of the transmitter receiver path.

Figure 3) The evolution of the power spectra of the received cw tone from one of the antenna/frequency sets, from 1840 Local Time to 2045 Local Time, August 10, 1990. The multiple peaks seen at early times are due to multiple hops on the 702 kilometer path. The features and distortions appearing at 1500 seconds are probably due to the passage of a developing plume, and the general Doppler spread is due to the complete developmetnt of bottomside spread F.

Figure 4) Individual Doppler spectra at two times, before the onset of spread f (750s) and well into developed spread F (5750s). Note the sharp peaks from the multiple hops of the early data, as compared to the smeared spectrum from the spread F structures.

Figure 5) This figure illustrates the evolution of spatial coherence, for a 50 meter antenna seperation. During the early evening the coherence was the usual "nearly 1.0", but as spread F developed the coherence decreased until it was less than 0.5

Figure 6)This figure illustrates the evolution of frequency coherence, for channels initially seperated by 10 kHz. Note that prior to spread F onset the coherence was essentially 1.0, and dropped into the statistical noise by 3500 seconds. After 7000 seconds the seperation was changed to 1 kHz, inder which conditions the coherence became barely measurable.

Figure 7) A east-west scan by the Altair Radar, at 8:01:41 UT (1200 s), just prior to spread F onset. Note the smooth ionospere with no coherent structures. The spectragram in Figure 3 shows unperturbed coherent reflections from this ionosphere.

Figure 8) Siilar to figure 7, taken at 8:47:20 (4000s) showing the beginning of low altitude coherent returns, and a plume reaching to high altitudes. The spectragram in Figure 3 shows structure probably due to this plume

Figure 9) Similar to figures 7 and 8, but showing well developed bottom side spread F. The spectragram in Figure 3 shows a wide Doppler spread, presumably from the mass of chaotic spread F echoes

Map of HF Propagation Path

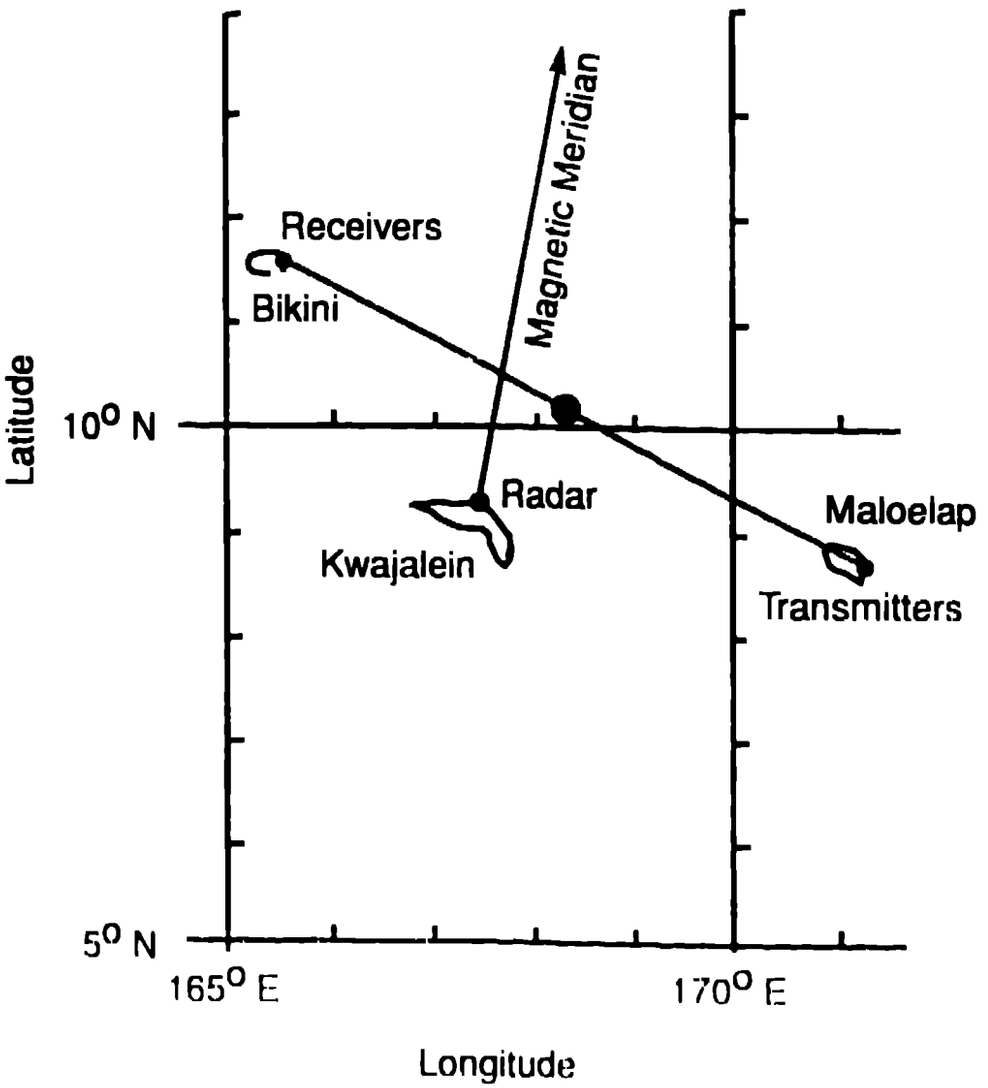

Figure 1

Geometry of Receive Antenna Array

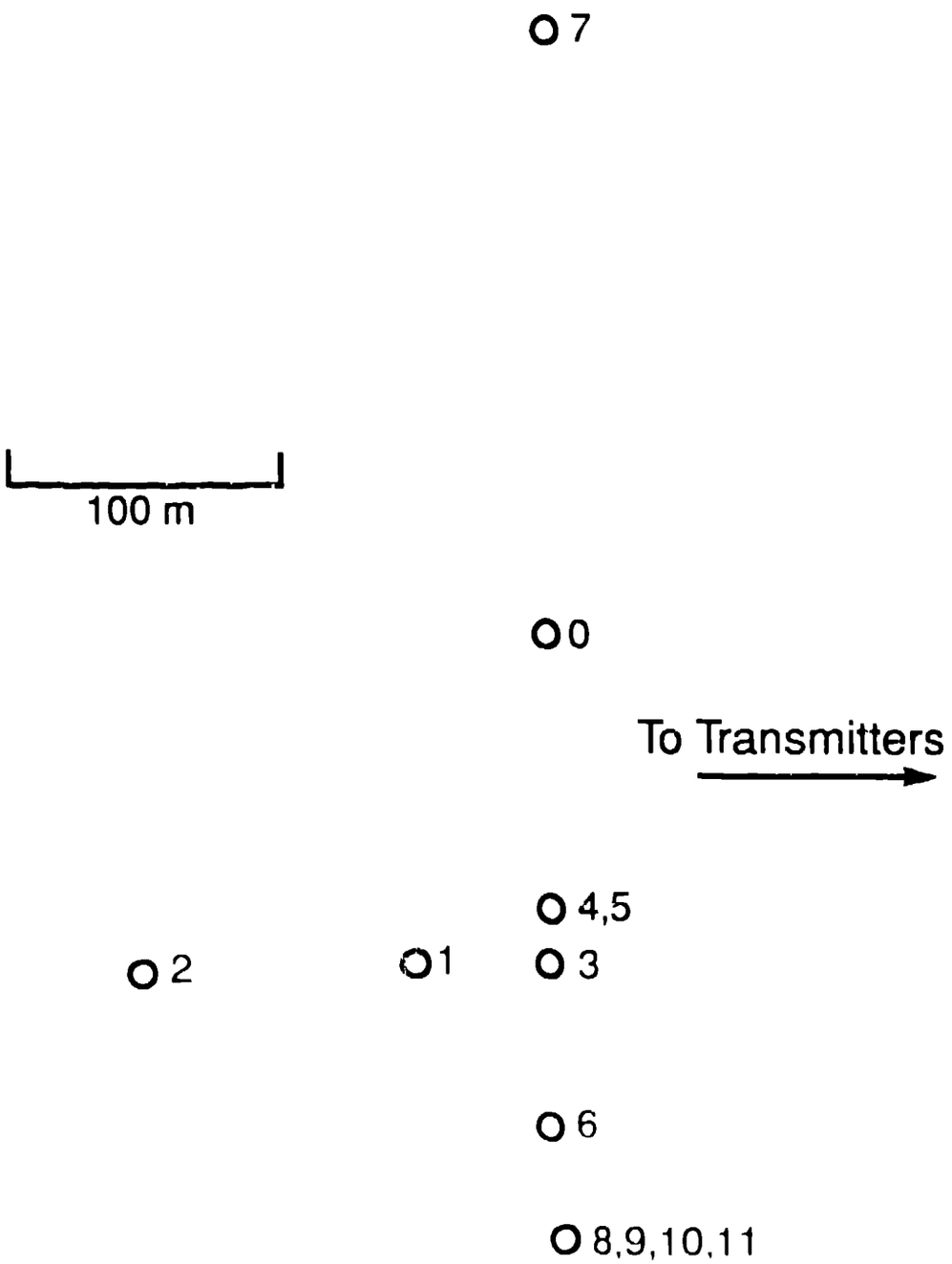

Figure 2

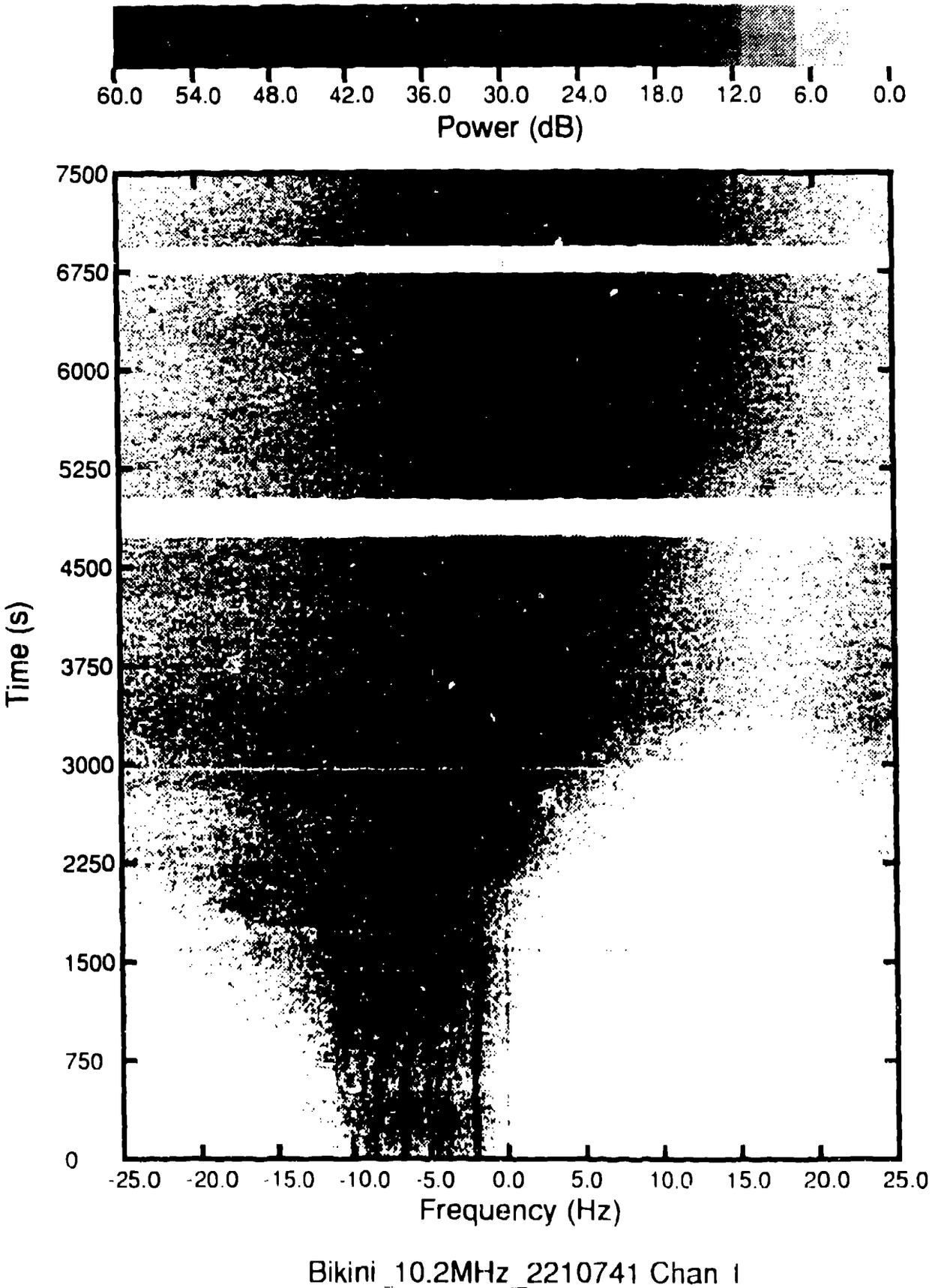
60.0
54.0
48.0
42.0
36.0
30.0
24.0
18.0
12.0
6.0
0.0
Power (dB)
7500
6750
6000
5250
4500
3750
3000
2250
1500
750
0
Time (s)
-25.0
-20.0
-15.0
-10.0
-5.0
0.0
5.0
10.0
15.0
20.0
25.0
Frequency (Hz)
Bikini_10.2MHz_2210741 Chan 1

Figure 3

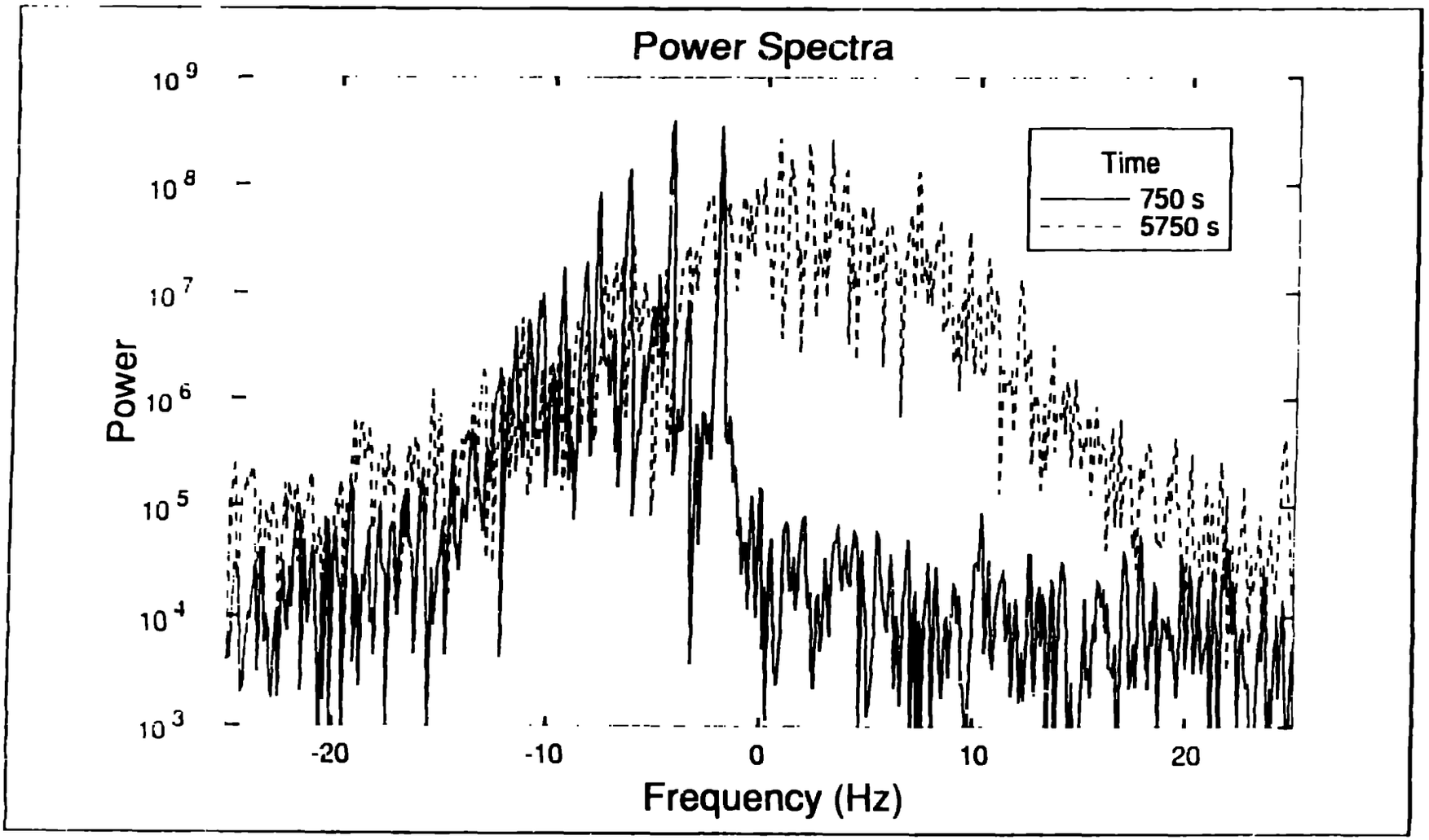
Power Spectra
Time
750 s
5750 s
Power
10^9
10^8
10^7
10^6
10^5
10^4
10^3
-20
-10
0
10
20
Frequency (Hz)

Figure 4

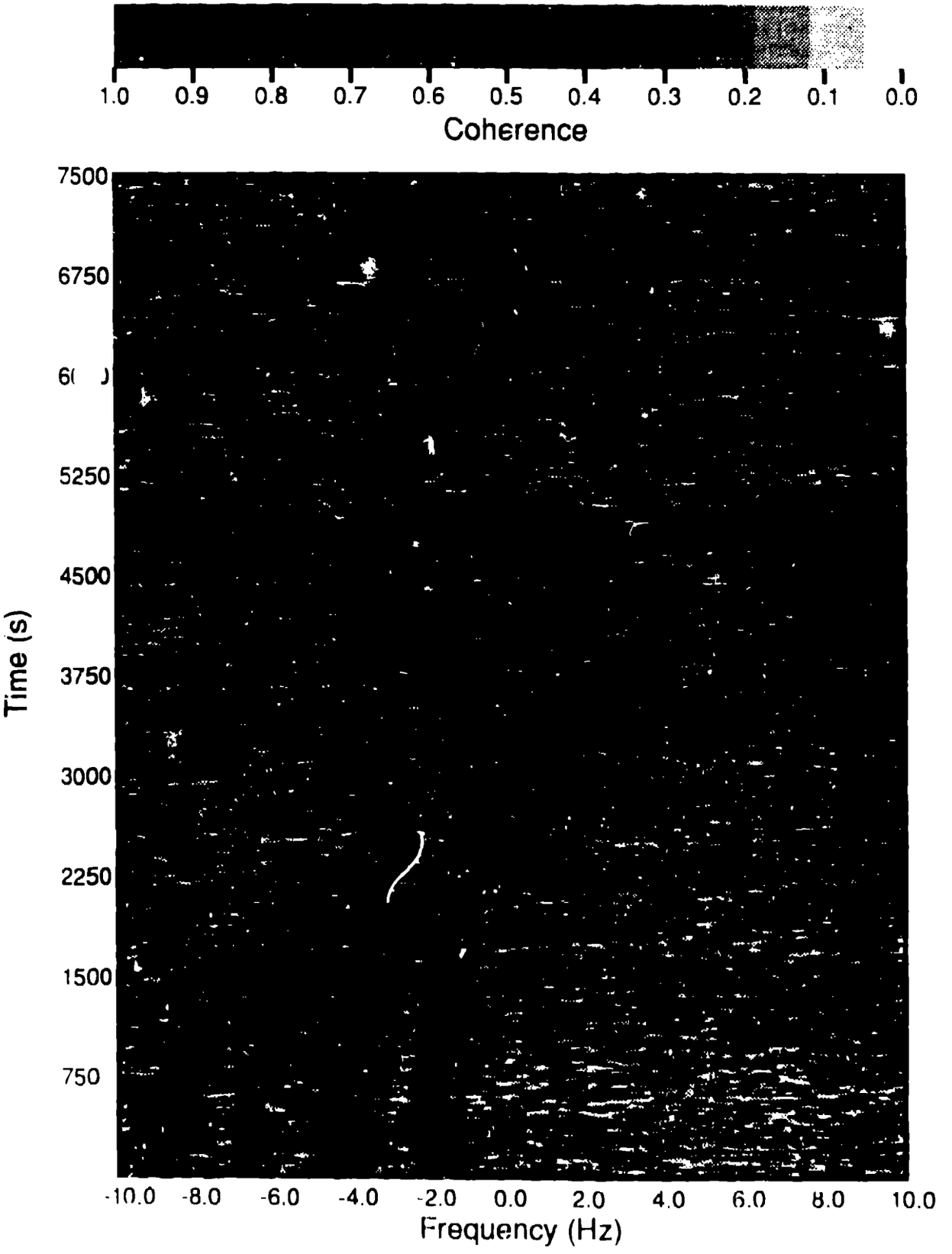
1.0
0.9
0.8
0.7
0.6
0.5
0.4
0.3
0.2
0.1
0.0
Coherence
7500
6750
6( )
5250
4500
3750
3000
2250
1500
750
Time (s)
-10.0
-8.0
-6.0
-4.0
-2.0
0.0
2.0
4.0
6.0
8.0
10.0
Frequency (Hz)
Bikini_10.2MHz_2210741 Chan 1-3

Figure 5

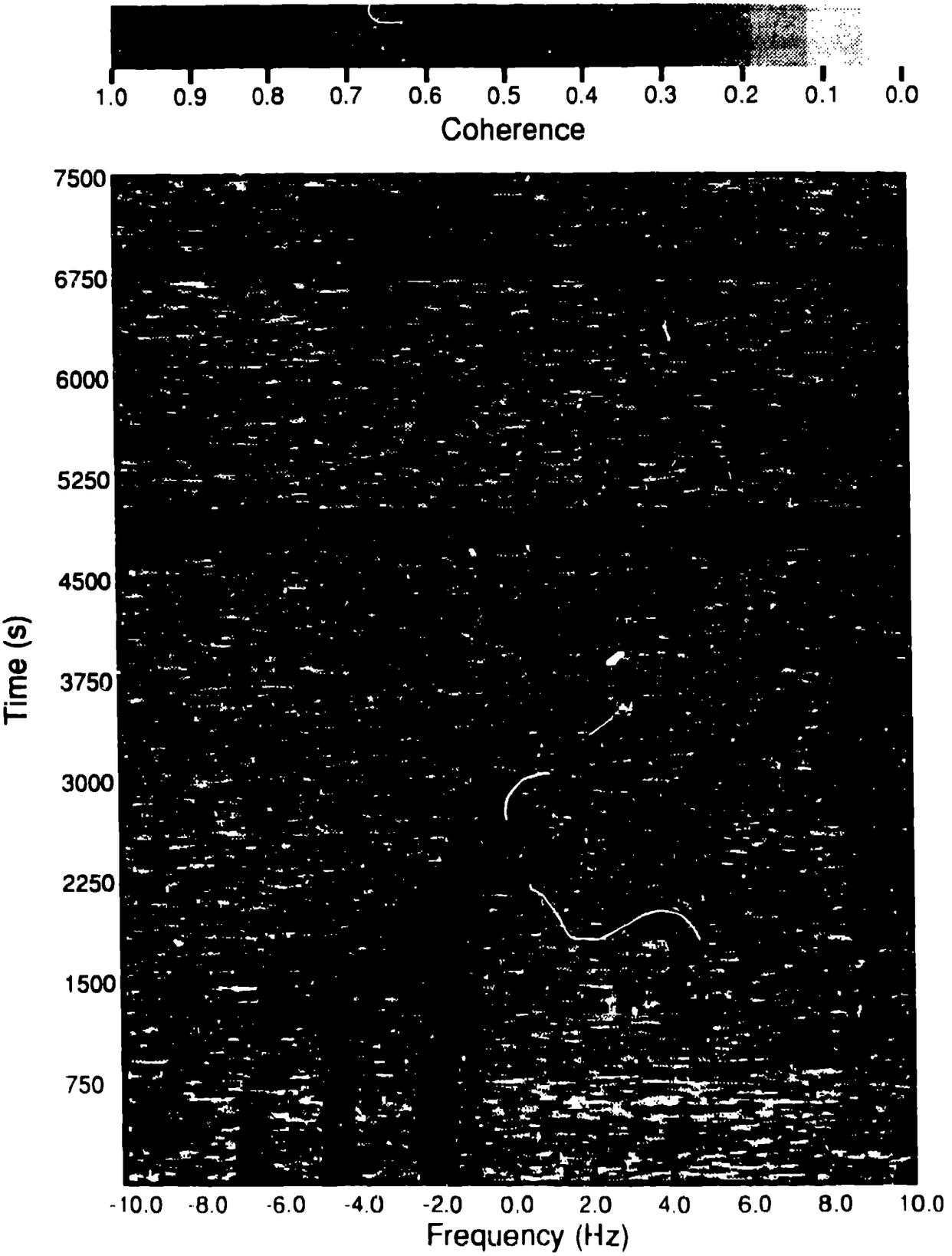
1.0
0.9
0.8
0.7
0.6
0.5
0.4
0.3
0.2
0.1
0.0
Coherence
7500
6750
6000
5250
4500
3750
3000
2250
1500
750
Time (s)
-10.0
-8.0
-6.0
-4.0
-2.0
0.0
2.0
4.0
6.0
8.0
10.0
Frequency (Hz)
Bikini_10.2MHz_2210741 Chan 8-9

Figure 6

Figure 7

Figure 8

Figure 9